Supplementary information for

Endophilin A2 deficiency protects rodents from autoimmune arthritis by modulating T cell activation

Authors:

Ulrika Norin*[1], Carola Rintisch[2,1], Liesu Meng[1,3], Florian Forster[1], Diana Ekman[4], Jonatan Tuncel[1], Katrin Klocke[1], Johan Bäcklund[1], Min Yang[1], Michael Y. Bonner[1], Gonzalo Fernandez Lahore[1], Klementy Shchetynsky[5], Maria Bergquist[6], Inger Gjertsson[6], Norbert Hubner[2,7], Liselotte Bäckdahl[1], Rikard Holmdahl*[1,3]

* Corresponding authors

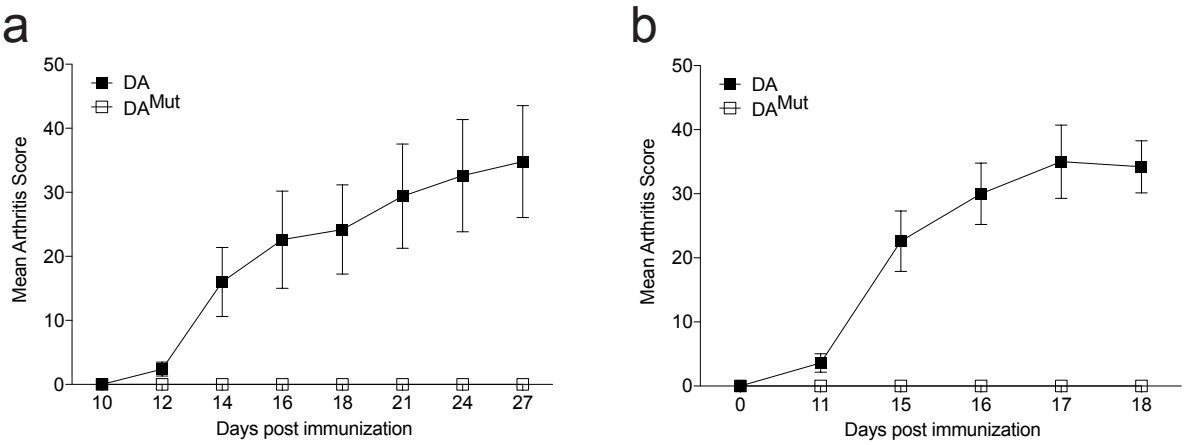

Supplementary figure 1. Arthritis resistance in DA^{Mut} rat is not due to environmental factors. a) Mean arthritis score in 5 DA and 7 DA^{Mut} rats after pristane immunization in conventional animal facility. b) Mean arthritis score in 5 DA and 4 DA^{Mut} rats after pristane immunization in SPF (FELASA II) animal facility. Data are presented as mean with error bars indicating ±SEM with each dot representing an individual value.

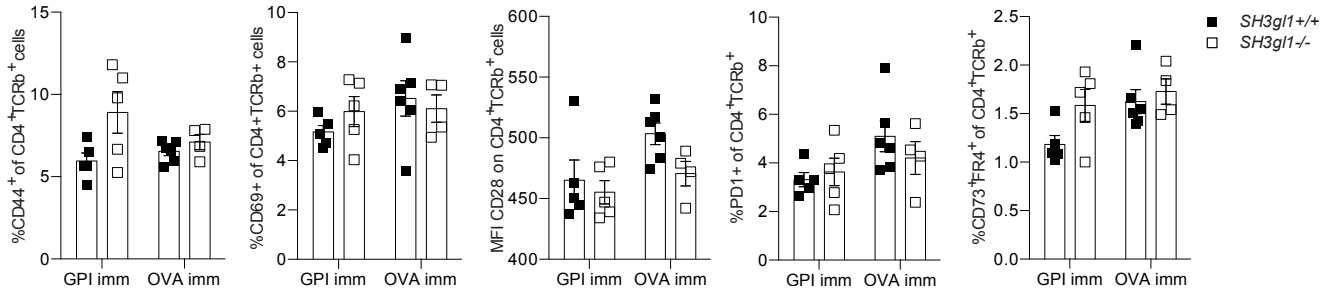

Supplementary figure 2. No difference in activated and anergic T cells after GPI-protein and ovalbumin immunization. Frequency and mean fluorescence intensity of activation and anergy markers in CD4+T cells from draining lymph nodes ten days after immunization with GPI protein (5 *SH3gl1* deficient mice and 4 wild type littermates) and ovalbumin (4 *SH3gl1* deficient mice and 6 wild type littermates). Data are presented as mean with error bars indicating ±SEM with each dot representing an individual value.

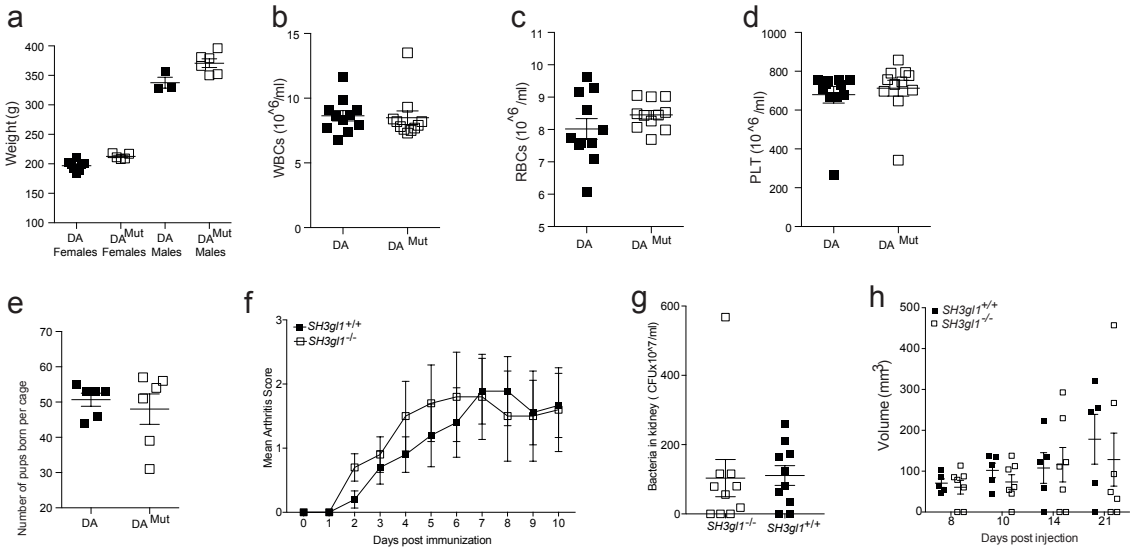

Supplementary figure 3. EA2 deficiency does not affect the general health of rodents or leads to increased susceptibility to a bacterial infection nor excessive tumor growth. a) Weight of DA and DA^{Mut} rats at 1.5 years of age b) Number of white blood cells (WBCs) in heparinized blood of 11 DA and 11 DA^{Mut} rats at 1.5 years of age c) Number of red blood cells (RBCs) in heparinized blood of DA and DA^{Mut} rats at 1.5 years of age d) Number of platelets in heparinized blood of DA and DA^{Mut} rats at 1.5 years of age e) Number of pups born from 6 individual DA and DA^{Mut} breeding pairs during a period of approximately one year. f) Mean arthritis score after induction of septic arthritis using *Staphylococcus aureus* LS-1 in 10 *Sh3gl1* deficient and 10 wildtype littermate mice. g) Colony-forming units in kidneys ten days after *Staphylococcus aureus* LS-1 infection. h) Tumor growth in 7 *SH3gl1* deficient mice and 5 wild type littermates after injection of melanoma cells. Data are presented as mean with error bars indicating ±SEM with each dot representing an individual value.

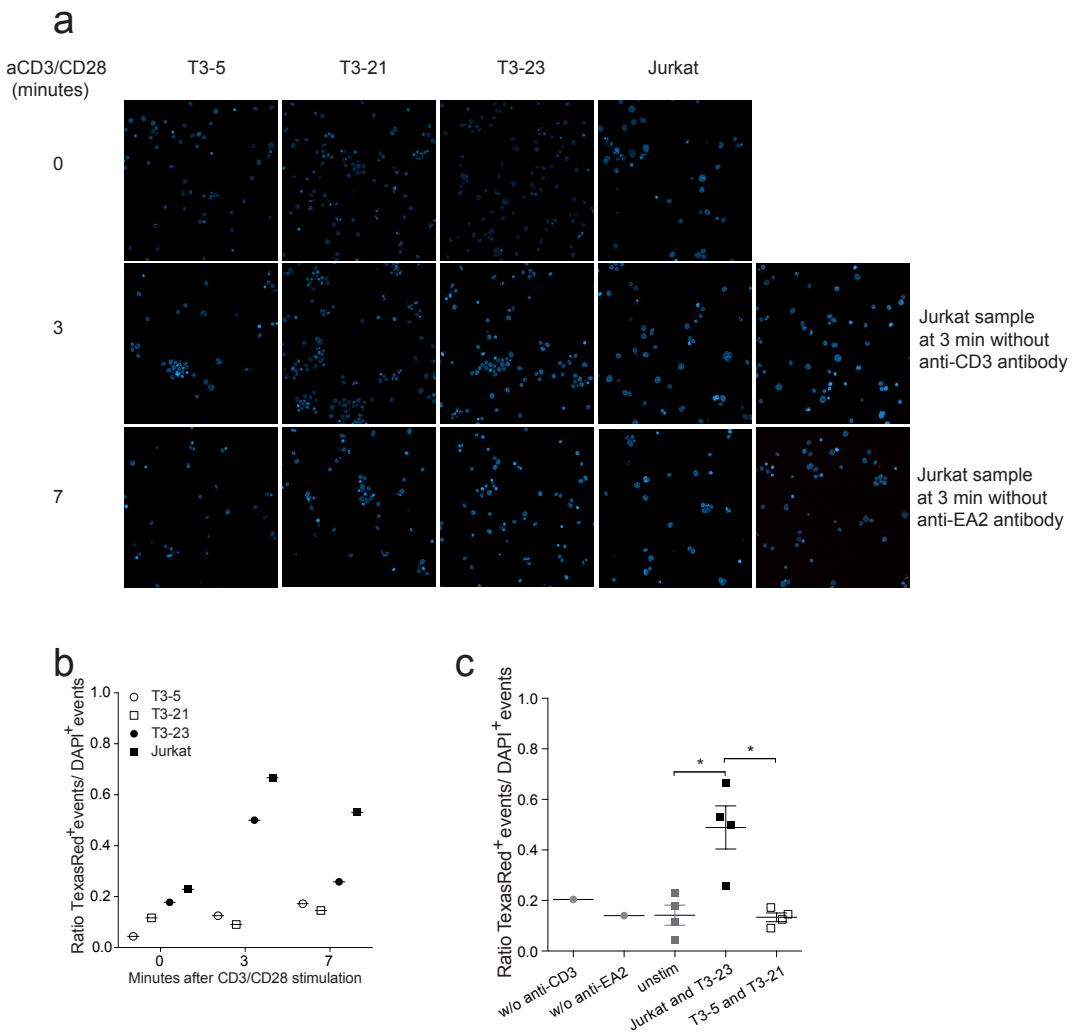

Supplementary figure 4. Co-localization of EA2 and the TCR in Jurkat and EA2 CRISPR knock-out cells. a) Detection of EA2 and TCR co-localization in unstimulated and anti-CD3/CD28 stimulated cells with proximity-ligase assay. b) Quantification of number of interactions determined as the ratio of TexasRed positive cells and DAPI positive cells in Jurkat and EA2 knock-out cells. c) Pooled ratio of TexasRed positive cells and DAPI positive cells from the three and seven-minute time points in *SHgl1* sufficient and *SH3gl1* deficient cells compared to the unstimulated samples. Non-parametrical Mann-Whitney *U* test was used for statistical evaluation of data. Data are presented as mean with error bars indicating ±SEM with each dot representing an individual value.

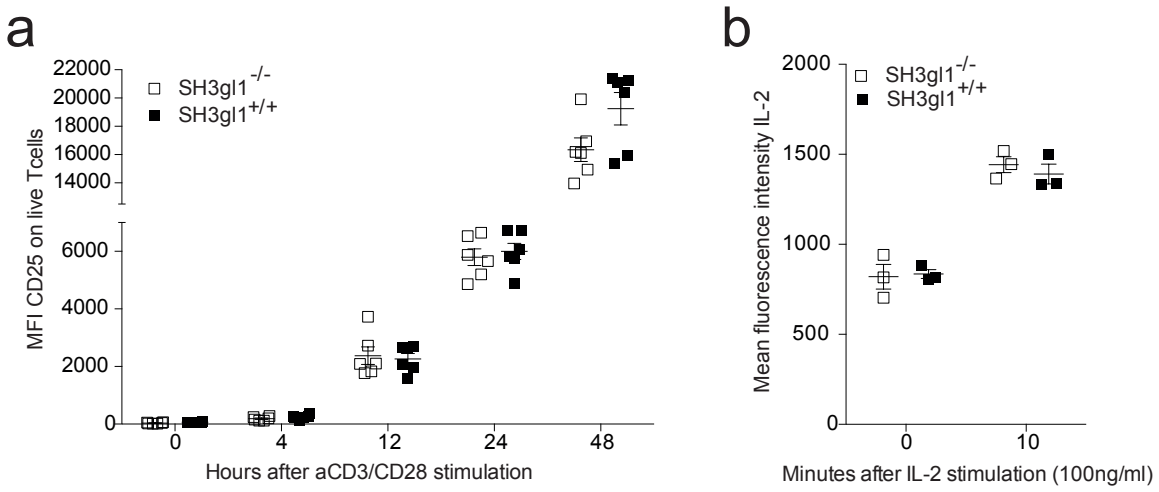

Supplementary figure 5. EA2 does not regulate activation induced CD25 expression nor IL-2 internalization. a) Expression of the IL-2 receptor CD25 after anti-CD3/CD28 stimulation in T cells from 6 *SH3gl1*$^{-/-}$ and 6 *SH3gl1*$^{+/+}$ mice. b) Expression of intracellular IL-2 in T cells before and 10 minutes after IL-2 stimulation in 3 *SH3gl1*$^{-/-}$ and 3 *SH3gl1*$^{+/+}$mice. Data are presented as mean with error bars indicating ±SEM with each dot representing an individual value.

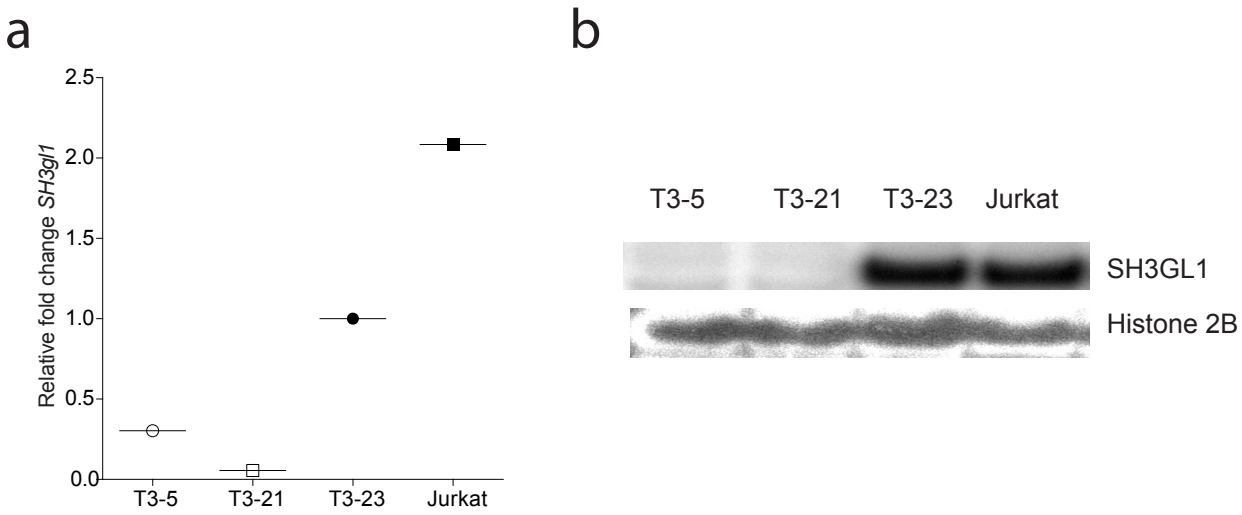

Supplementary figure 6. Knock-down efficacy of EA2 in EA2 CRISPR knock-out cells. a) *SH3gl1* gene expression in EA2 CRISPR Jurkat knock-out cells relative to normal Jurkat cells. b) Western blot analysis of the expression of the Endophilin A2 protein in EA2 CRISPR Jurkat knock-out cells. Histone 2B was used as loading control.

a

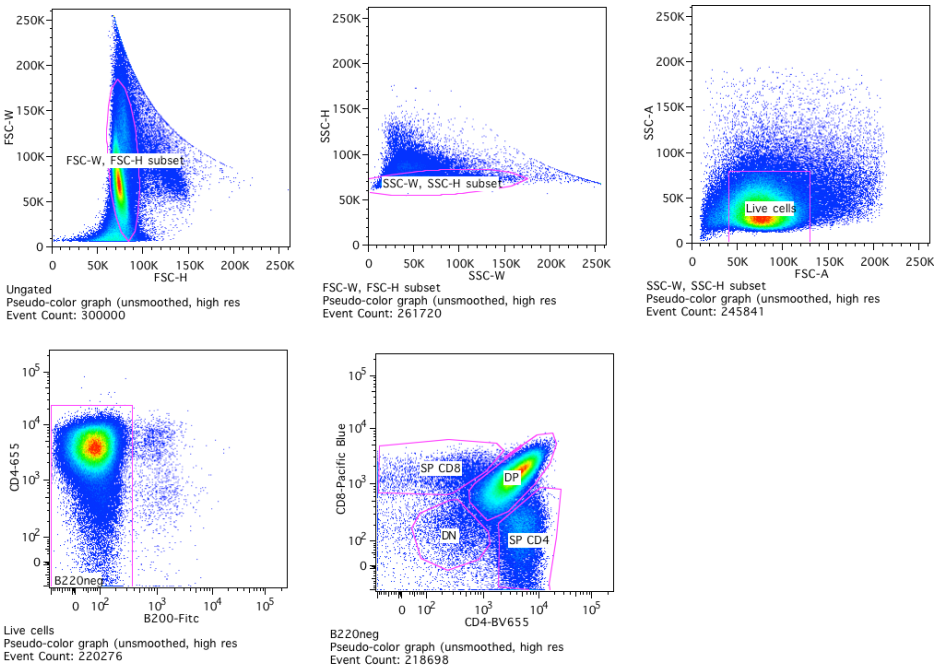
FSC-W, FSC-H subset
SSC-W, SSC-H subset
Live cells
SP CD8
DP
DN
SP CD4
B220neg
Ungated
Pseudo-color graph (unsmoothed, high res
Event Count: 300000
FSC-W, FSC-H subset
Pseudo-color graph (unsmoothed, high res
Event Count: 261720
SSC-W, SSC-H subset
Pseudo-color graph (unsmoothed, high res
Event Count: 245841
Live cells
Pseudo-color graph (unsmoothed, high res
Event Count: 220276
B220neg
Pseudo-color graph (unsmoothed, high res
Event Count: 218698

b

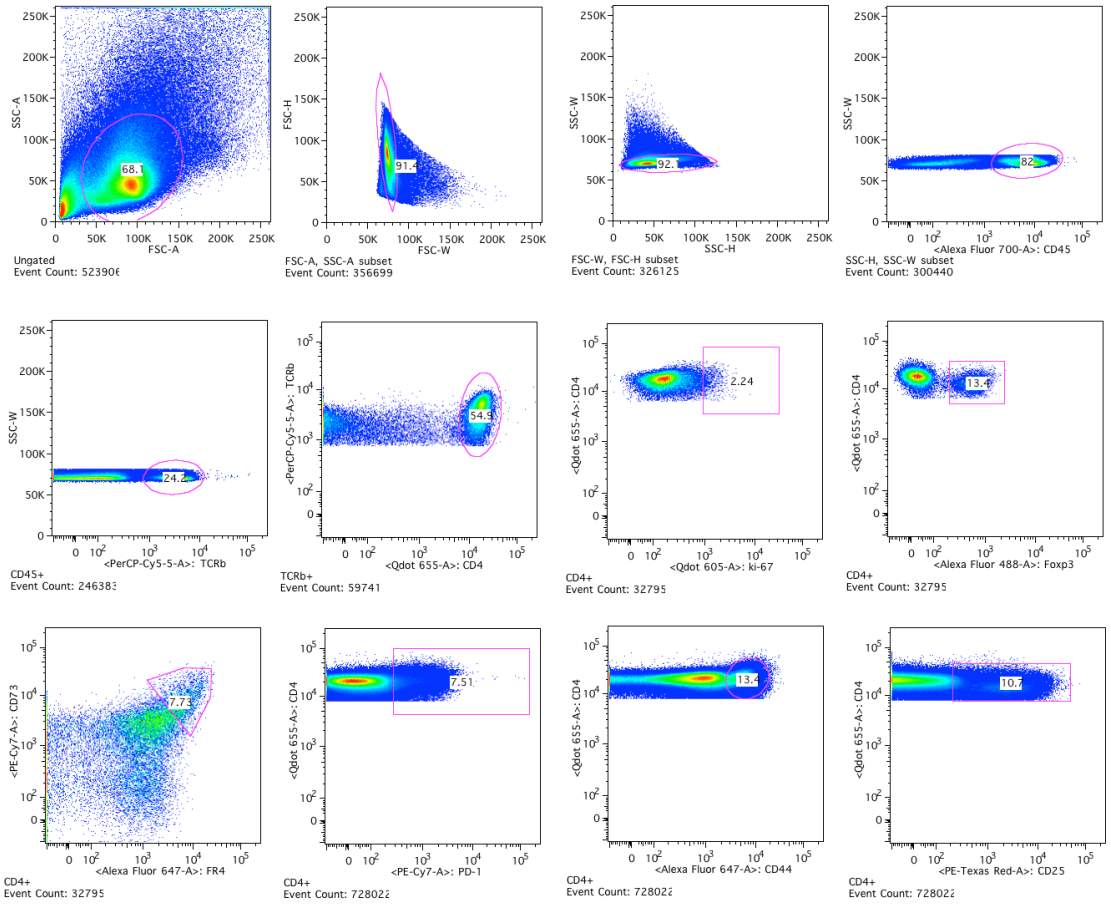
68.1
91.4
92.1
82
24.2
54.9
2.24
13.4
7.73
7.51
13.4
10.7
Ungated
FSC-A, SSC-A subset
Event Count: 356699
FSC-W, FSC-H subset
Event Count: 326125
SSC-H, SSC-W subset
Event Count: 300440
CD45+
TCRb+
CD4+
CD4+
CD4+
CD4+
CD4+

c

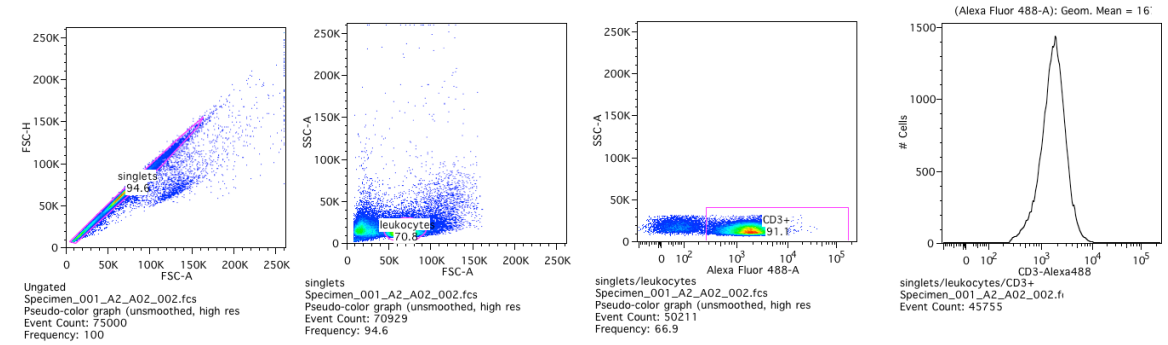
singlets
94.6
leukocytes
70.8
CD3+
91.1
(Alexa Fluor 488-A): Geom. Mean = 16
Ungated
Specimen_001_A2_A02_002.fcs
Pseudo-color graph (unsmoothed, high res
Event Count: 75000
Frequency: 100
singlets
Specimen_001_A2_A02_002.fcs
Pseudo-color graph (unsmoothed, high res
Event Count: 70929
Frequency: 94.6
singlets/leukocytes
Specimen_001_A2_A02_002.fcs
Pseudo-color graph (unsmoothed, high res
Event Count: 50211
Frequency: 66.9
singlets/leukocytes/CD3+
Specimen_001_A2_A02_002.fc
Event Count: 45755

d

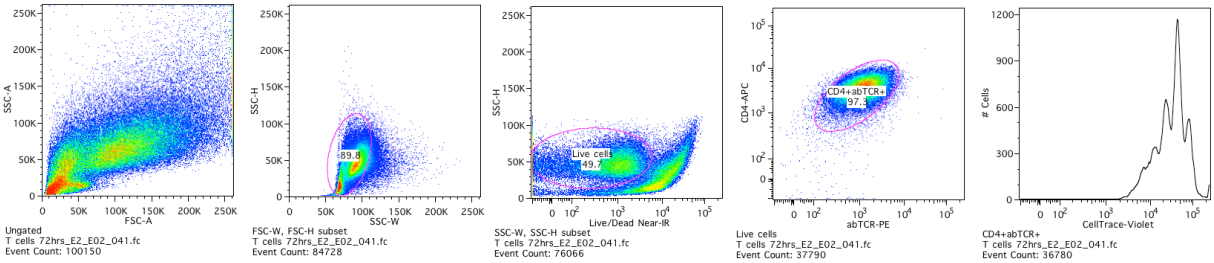
89.8
Live cells
49.7
CD4+abTCR+
97.1
Ungated
T cells 72hrs_E2_E02_041.fc
Event Count: 100150
FSC-W, FSC-H subset
T cells 72hrs_E2_E02_041.fc
Event Count: 84728
SSC-W, SSC-H subset
T cells 72hrs_E2_E02_041.fc
Event Count: 76066
Live cells
T cells 72hrs_E2_E02_041.fc
Event Count: 37790
CD4+abTCR+
T cells 72hrs_E2_E02_041.fc
Event Count: 36780

e

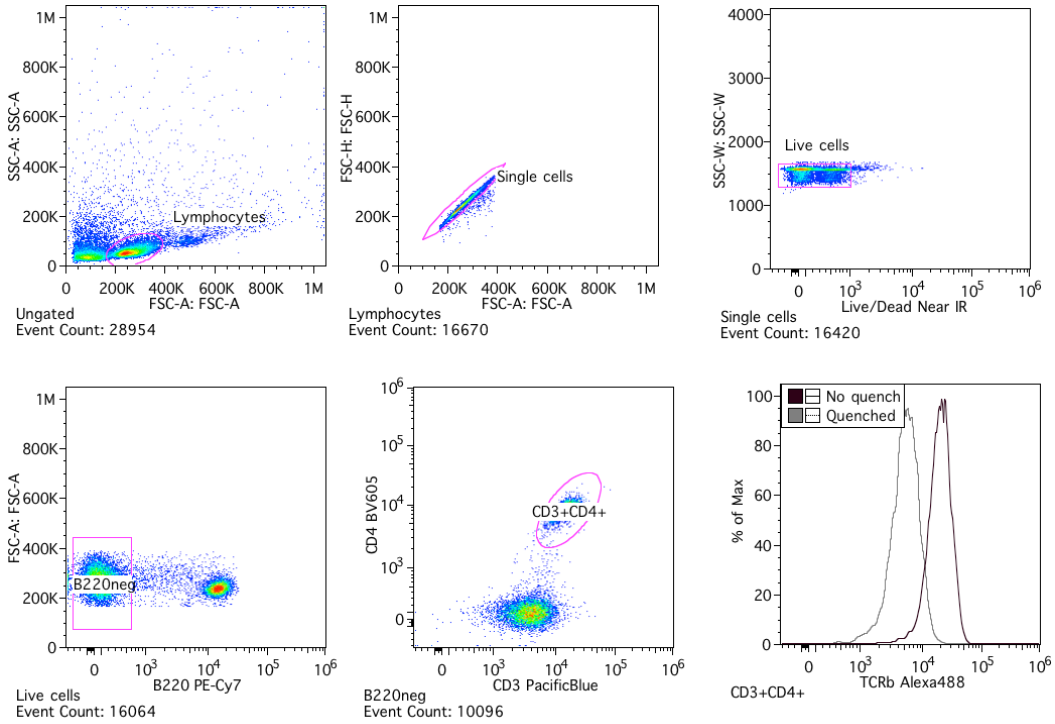
Lymphocytes
Single cells
Live cells
B220neg
CD3+CD4+
No quench
Quenched
Ungated
Event Count: 28954
Lymphocytes
Event Count: 16670
Single cells
Event Count: 16420
Live cells
Event Count: 16064
B220neg
Event Count: 10096
CD3+CD4+

f

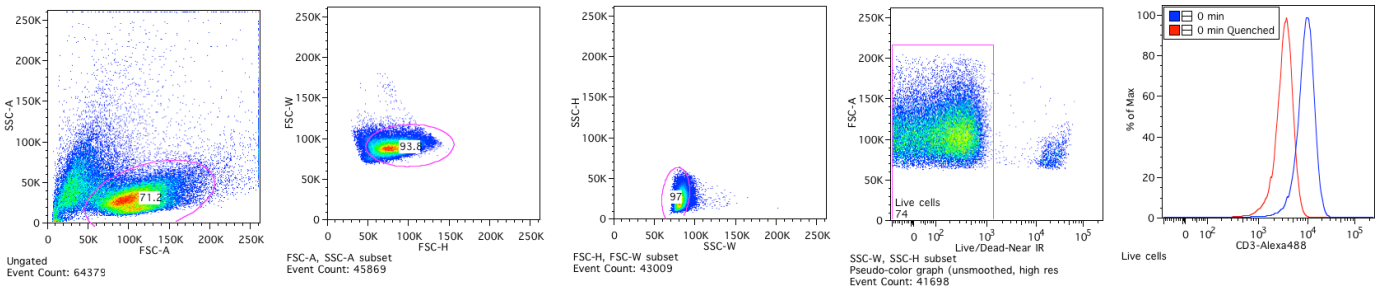
SSC-A
FSC-A
71.2
Ungated
Event Count: 64379
FSC-W
FSC-H
93.8
FSC-A, SSC-A subset
Event Count: 45869
SSC-H
SSC-W
97
FSC-H, FSC-W subset
Event Count: 43009
FSC-A
Live/Dead-Near IR
Live cells
74
SSC-W, SSC-H subset
Pseudo-color graph (unsmoothed, high res
Event Count: 41698
0 min
0 min Quenched
% of Max
CD3-Alexa488
Live cells

g

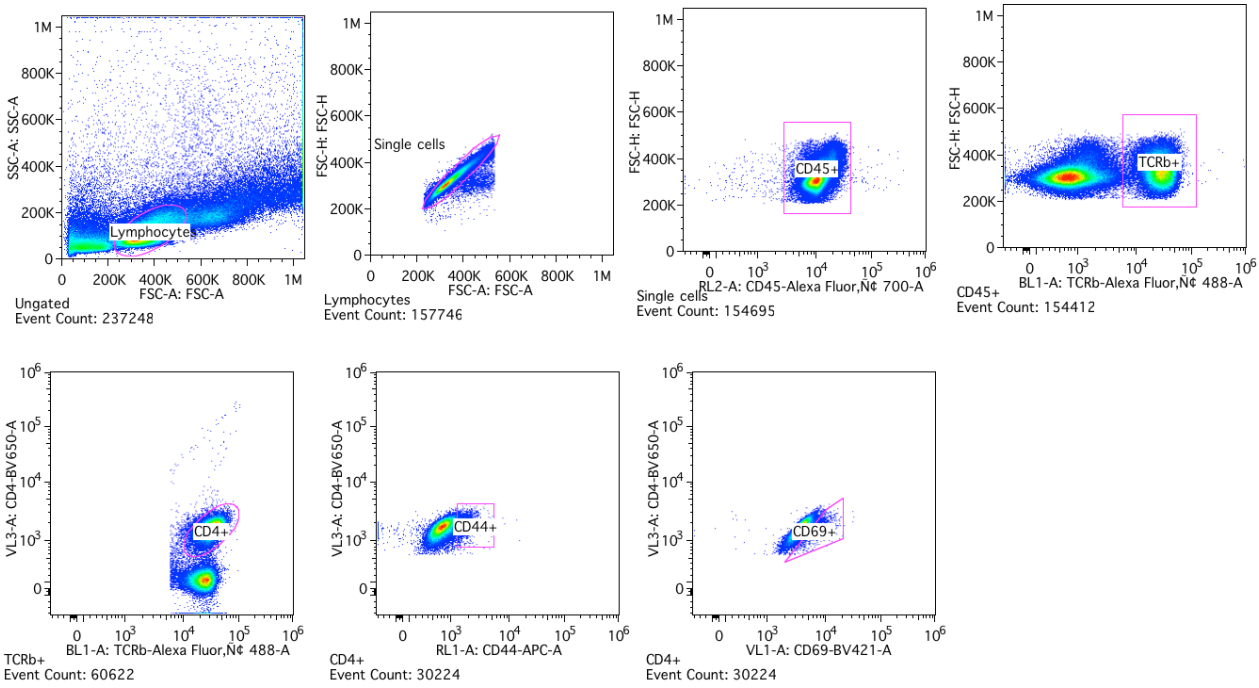
SSC-A: SSC-A
FSC-A: FSC-A
Lymphocytes
Ungated
Event Count: 237248
FSC-H: FSC-H
Single cells
Lymphocytes
Event Count: 157746
CD45+
RL2-A: CD45-Alexa Fluor,N¢ 700-A
Single cells
Event Count: 154695
TCRb+
BL1-A: TCRb-Alexa Fluor,N¢ 488-A
CD45+
Event Count: 154412
VL3-A: CD4-BV650-A
CD4+
BL1-A: TCRb-Alexa Fluor,N¢ 488-A
TCRb+
Event Count: 60622
CD44+
RL1-A: CD44-APC-A
CD4+
Event Count: 30224
CD69+
VL1-A: CD69-BV421-A
CD4+
Event Count: 30224

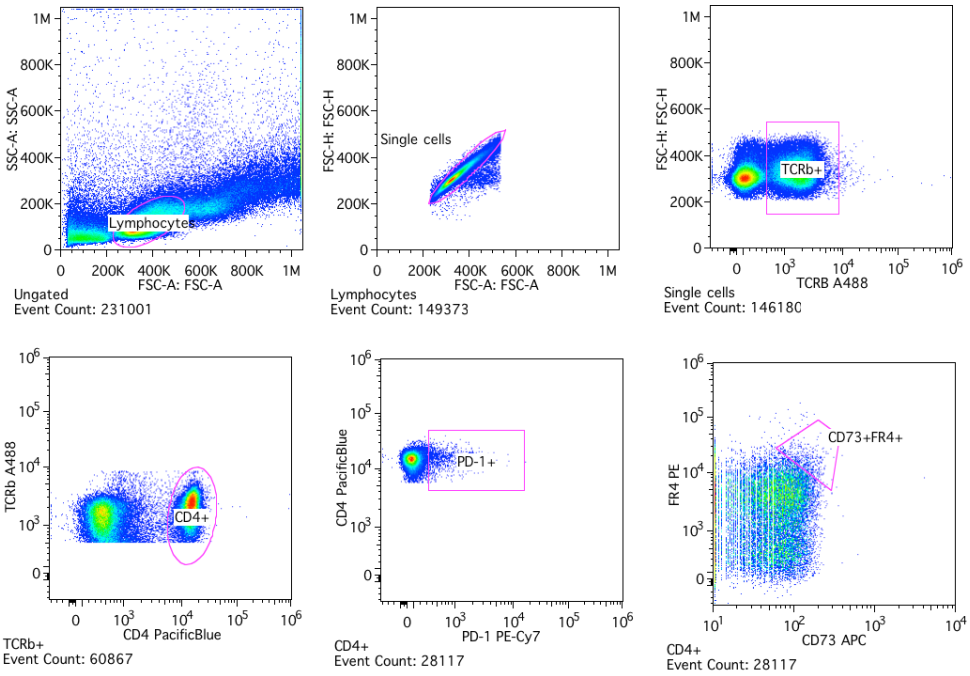
SSC-A: SSC-A
FSC-A: FSC-A
Lymphocytes
Ungated
Event Count: 231001
FSC-H: FSC-H
Single cells
Lymphocytes
Event Count: 149373
TCRb+
Single cells
Event Count: 146180
TCRb A488
CD4 PacificBlue
CD4+
TCRb+
Event Count: 60867
CD4 PacificBlue
PD-1 PE-Cy7
PD-1+
CD4+
Event Count: 28117
FR4 PE
CD73 APC
CD73+FR4+
CD4+
Event Count: 28117

h

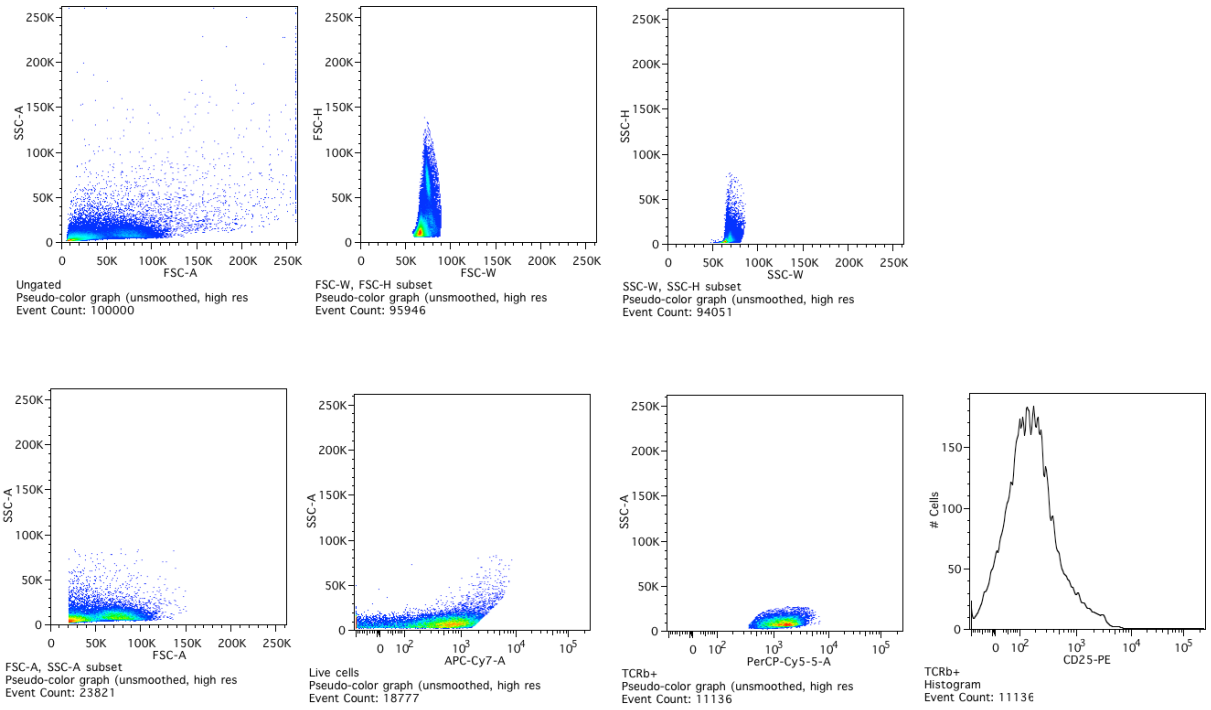
SSC-A
FSC-A
Ungated
Pseudo-color graph (unsmoothed, high res
Event Count: 100000
FSC-H
FSC-W
FSC-W, FSC-H subset
Pseudo-color graph (unsmoothed, high res
Event Count: 95946
SSC-H
SSC-W
SSC-W, SSC-H subset
Pseudo-color graph (unsmoothed, high res
Event Count: 94051
FSC-A, SSC-A subset
Pseudo-color graph (unsmoothed, high res
Event Count: 23821
APC-Cy7-A
Live cells
Pseudo-color graph (unsmoothed, high res
Event Count: 18777
PerCP-Cy5-5-A
TCRb+
Pseudo-color graph (unsmoothed, high res
Event Count: 11136
Cells
CD25-PE
TCRb+
Histogram
Event Count: 11136

i

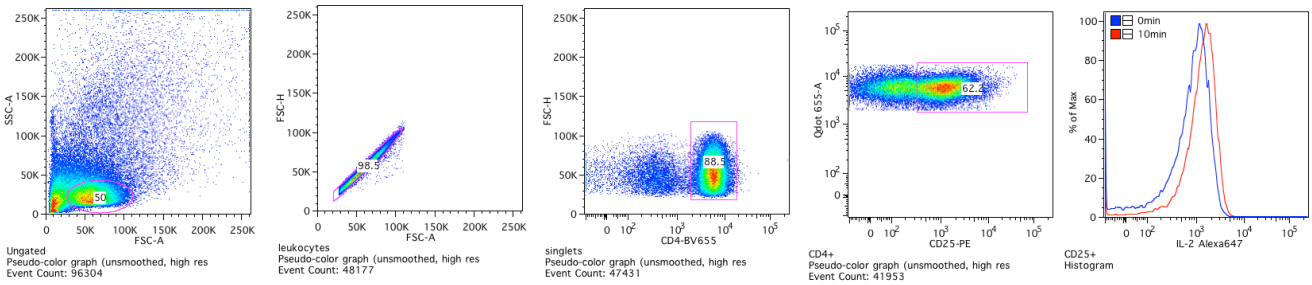

Supplementary figure 7. Representative FlowJo plots displaying stepwise gating strategy for flow cytometry analysis with subsequent number of cells analyzed within each gate. a) Gating strategy for thymocyte populations shown in Figure 3e. b) Gating strategy for identification of T cell activation and anergy shown in Figure 3f c) Gating strategy for TCR internalization in rat T cells shown in Figure 4b d) Gating strategy for identification of proliferation of T cells shown in Figure 4f e) Gating strategy for TCR internalization in T cells from lymph nodes shown in Figure 4i f) Gating strategy for TCR internalization in CRISPR Jurkat T cells shown in Figure 5a g) Gating strategy for identification of T cell activation and anergy shown in Supplementary figure 2 h) Gating strategy for identification of expression of CD25 on T cells shown in Supplementary figure 5a i) Gating strategy for identification of intracellular levels of IL-2 shown in Supplementary figure 5b

Supplementary Table 1. Sequences of PCR primers used for H3K4me3 and H4ac ChIP-qPCR

Gene	Primer set	Forward primer	Reverse primer
Gapdh	1	TACTTCGGCCACCCTATCCA	CATGCCGGTCTGGCTAAATT
Sh3gl1	1	CGAGAAACTGAACTCCGGATCT	GGAACGAATGGTTCTCCAGTTAA
Sh3gl1	2	CGGAAACCTTAGTTCGAGCG	AACTGCTTCTTCAGCCCCG
Sh3gl1	3	CAGGCCACAGAAAATGTTTGTC	GCCCTGTGCAGACTTGGTAAG